Chelate and Bridge Diphosphine Isomerization: Triosmium and Triruthenium Clusters Containing 1,1′-Bis(diphenylphosphino)ferrocene (dppf)

Noorjahan Begum,[†] Uttam K. Das,[†] Manzur Hassan,[†] Graeme Hogarth,*[,‡] Shariff E. Kabir,*[,†] Ebbe Nordlander,[§] Mohammad A. Rahman,[†] and Derek A. Tocher*[,‡]

Department of Chemistry, Jahangirnagar University, Savar, Dhaka-1342, Bangladesh, Department of Chemistry, University College London, 20 Gordon Street, London WC1H OAJ, UK, and Inorganic Chemistry Research Group, Chemical Physics, Center for Chemistry and Chemical Engineering, Lund University, Box 124, SE-221 00 Lund, Sweden

Received July 26, 2007

The coordination mode of dppf {dppf = 1,1′-bis(diphenylphosphino)ferrocene} at triosmium and triruthenium carbonyl clusters has been studied. Heating $[Os_3(CO)_{12}]$ with dppf in the presence of Me_3NO in benzene at 60 °C furnishes three triosmium compounds, $[Os_3(CO)_{11}(\kappa^1\text{-dppf})]$ (**1**), $[Os_3(CO)_{10}(\kappa^2\text{-dppf})]$ (**2**), and $[Os_3(CO)_{10}(\mu\text{-dppf})]$ (**3**) in 10, 20, and 30% yields, respectively. Reaction of the labile cluster $[Os_3(CO)_{10}(MeCN)_2]$ with dppf at room temperature also gives **1**, **2**, and **3** (5, 10, and 35% yields). Treatment of **1**, which contains a pendant diphosphine, with Me_3NO at room temperature affords **2** via a ring closure reaction, whereas heating **2**, in which the dppf ligand is chelating, at 110 °C affords the thermodynamically stable bridging isomer **3**, in which phosphorus atoms are bound at equatorial positions. Reaction of the unsaturated cluster $[Os_3(CO)_{10}(\mu\text{-H})_2]$ (**4**) with dppf in refluxing THF affords the bridging complex $[Os_3(CO)_8(\mu\text{-dppf})(\mu\text{-H})_2]$ (**6**) in high yield as the sole product. Hydrogenation of **3** with H_2 at 110 °C at 1 atm also yields **6**. Reactions of both the saturated $[Os_3(CO)_{10}(\mu\text{-dppm})]$ (**7**) and electron-deficient $[Os_3(CO)_8\{\mu_3\text{-}Ph_2PCH_2P(Ph)C_6H_4\}(\mu\text{-H})]$ (**8**) with dppf at 110 °C and at room temperature respectively yield $[Os_3(CO)_9(\mu\text{-dppm})(\kappa^1\text{-dppf})]$ (**9**) and $[Os_3(CO)_8(\mu\text{-dppm})(\kappa^2\text{-dppf})]$ (**10**). Compound **9** converts to **10** at 110 °C via CO loss and phosphorus coordination. Reaction of $[Ru_3(CO)_{12}]$ with dppf in the presence of Me_3NO affords the dihydroxy-bridged complex, $[Ru_3(CO)_8(\mu\text{-dppf})(\mu\text{-OH})_2]$ (**13**), together with the previously reported compounds $[Ru_3(CO)_{10}(\mu\text{-dppf})]$ (**11**) and $[Ru_3(CO)_8(\mu\text{-dppf})_2]$ (**12**).

Introduction

In the past two decades, there has been considerable advances in the synthesis and reactivity of transition metal complexes bearing diphosphine ligands due to their potential applicability to effect organic transformations,[1] their ability to act as templates for the synthesis of metal−metal bonds by bridge-assisted reactions,[2−6] and their widespread application in homogeneous catalysis.[7−11] When metal bound, diphosphines can coordinate in monodentate, chelating, or bridging modes, and interconversions between these often result from slight changes in the ligand backbone or in co-ligands bound to the metal center(s).[12] Chelate-bridge isomerization of diphosphine ligands on metal complexes that are not accompanied by the addition and elimination of other ligands is a property that may be associated with homogeneous catalysis. In polynuclear complexes, the small bite-angle diphosphine, bis(diphenylphosphino)methane (dppm), can act as a chelate ligand, but the four-membered rings generated are strained, and thus it has a greater tendency to act in either a monodentate or a bridging bidentate mode,[13] the latter giving dinuclear complexes that can provide suitable reactive sites to facilitate the simultaneous activation of substrate molecules.[1] In contrast, 1,2-bis(diphenylphosphino)ethane (dppe) is an excellent chelating ligand, although less commonly it is known to bridge metal−metal bonds.[13]

The reactions of $[Os_3(CO)_{12}]$ and activated derivatives $[Os_3(CO)_{11}(MeCN)]$, $[Os_3(CO)_{10}(MeCN)_2]$, and $[Os_3(CO)_{10}(cis\text{-}C_4H_6)]$ with diphosphines were first investigated in the mid-

* To whom correspondence should be addressed. E-mail: g.hogarth@ucl.ac.uk.

[†] Jahangirnagar University.

[‡] University College London.

[§] Lund University.

(1) Miyake, Y.; Nomaguchi, Y.; Yuki, M.; Nishibayashi, Y. *Organometallics* **2007**, *26*, 3611.

(2) Fan, W.; Zhang, R. Leong, W. K.; Yan, Y. K. *Inorg. Chim. Acta* **2004**, *357*, 2441.

(3) Adatia, T.; Console, G.; Drake, S. R.; Johnson, B. F. G.; Kessler, M.; Lewis, J.; McPartlin, M. *J. Chem. Soc., Dalton Trans*. **1997**, 669.

(4) Adatia, T.; Brown, S. S. D.; Slater, I. D. *J. Chem. Soc., Dalton Trans.* **1993**, 559.

(5) Brown, M. P.; Dolby, P. A.; Harding, M. M.; Mathews, A.; Smith, A. *J. Chem. Soc., Dalton Trans*. **1993**, 559.

(6) Braga, D.; Matteoli, U.; Sabatino, P.; Scrivanti, A. *J. Chem. Soc., Dalton Trans*. **1995**, 419.

(7) Diz, E. L.; Neels, A.; Stoeckli-Evans, H.; Süss-Fink, G. *Polyhedron* **2001**, *20*, 2771.

(8) Kuiper, J. L.; Shapley, P. A.; Rayner, C. M. *Organometallics* **2004**, *23*, 3814.

(9) Dennett, J. N. L.; Gillon, A. L.; Heslop, K.; Hyett, D. J.; Fleming, J. S.; Lioyd-Jones, C. E.; Orpen, A. G.; Pringle, P. G.; Wass, D. F.; Scutt, J. N.; Weatherhead, R. H. *Organometallics* **2004**, *23*, 6078.

(10) Albers, I.; Alvarez, J.; Campora, J.; Maya, C. M.; Palma, P.; Sanchez, L. J.; Passaglia, *J. Organomet. Chem*. **2004**, *689*, 833.

(11) Marr, A. C.; Nieuwenhuyzen, M.; Pollock, C. L.; Saunders, G. C. *Organometallics* **2007**, *26*, 2659.

(12) Gallo, V.; Mastrorilli, P.; Nobile, C. F.; Braunstein, P.; Englert, U. *Dalton Trans.* **2006**, 2342.

(13) (a) Puddephatt, R. J. *Chem. Soc. Rev.* **1983**, *12*, 99. (b) Chaudret, B.; Delavaux, B.; Poilblanc, R. *Coord. Chem. Rev.* **1988**, *86*, 191.

10.1021/om700759z CCC: $37.00
Publication on Web 10/31/2007

Scheme 1

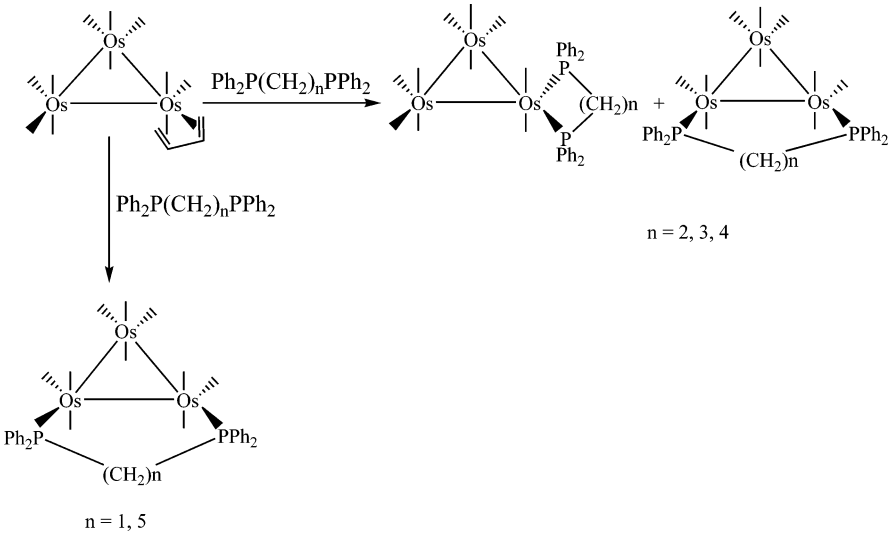

1980s. Poë and Sekhar[14] reported the formation of $[Os_3(CO)_{11}(\kappa^1\text{-dppm})]$, obtained from the room-temperature reaction of $[Os_3(CO)_{11}(MeCN)]$ with dppm, which subsequently undergoes ring-closure at 60−70 °C to afford the bridging diphosphine complex $[Os_3(CO)_{10}(\mu\text{-dppm})]$. In related work, Smith et al.[15] also reported the synthesis of $[Os_3(CO)_{10}(\mu\text{-dppm})]$ from the Me_3NO initiated reaction of $[Os_3(CO)_{12}]$ with dppm. We have also prepared this product from the reaction of dppm and $[Os_3(CO)_{10}(cis\text{-}C_4H_6)]$ at 68 °C.[16] In the latter, the butadiene is bound to a single metal atom, and this is important since it suggests that the anticipated chelate isomer is either too strained to be stable or rearranges rapidly to the favored bridging conformation. This prompted us to explore the effect of the length of diphosphine backbone as well as the structure of starting clusters on the formation of chelating versus bridging isomers of $[Os_3(CO)_{10}\{Ph_2P(CH_2)_nPPh_2\}]$ ($n = 1-5$).[16] Thus, whereas dppm exclusively bridges a metal−metal vector, dppe predominantly forms the chelating complex, the bridging isomer being only a minor product. Interestingly, we observed that the chelating tendency decreases as the chain length increases, so for 1,5-bis(diphenylphosphino)pentane (dpppe), only the bridging isomer was obtained (Scheme 1).[16−18] It is likely that steric effects will have a major influence on the bridging versus chelating behavior of these ligands.

Suitable ligand choice is clearly an important factor when constructing a desired multinuclear skeleton with bridge/chelate diphosphine. Recently, Richmond's group have carried out intensive studies, on bridge-chelate isomerization of diphosphines at the triosmium center, detailing kinetic aspects of the process as well as subsequent carbon−hydrogen and phosphorus−carbon bond cleavage reactions of the rigid and unsaturated diphosphines *cis*-$Ph_2PCH{=}CHPPh_2$ (dppv),[19] 4,5-bis(diphenylphosphino)-4-cyclopentene-1,3-dione (bpcd),[20] and 2,3-bis(diphenylphosphinomethyl)-*N*-*p*-tolylmaleimide (bmi).[21] For example, with dppv, chelate and bridge isomers are in equilibrium, the former being favored by ca. 7:1 at room temperature,[19] a process that has been shown to be nondissociative in nature.

The flexible diphosphine, 1,1′-bis(diphenylphosphino)ferrocene (dppf), is an important member of the ferrocenylphosphine family that has found widespread use in a range of homogeneous catalytic processes.[22] These stem from its ability to adopt various coordination modes that can match the steric requirements of the existing molecular environment.[23−30] Most commonly, dppf chelates to a single metal atom, but it can also act as a monodentate ligand, as a bridge between disparate metal centers, or as a bridge across a metal−metal bond. Importantly for catalytic applications, when acting as a chelating ligand, it is tolerant to bite-angles ranging from 90° to over 120°, and this allows low-energy pathways for metal-centered transformations.[31] Dppf displays two types of conformational flexibility: a tilting motion of the two cyclopentadienyl ring planes thus changing their dihedral angle, and a torsional rotation around the axis passing through the two ring centroids, and these allow a wide range of bite-angles of dppf when bound to molecular clusters.[32−38]

(14) Poë, A.; Sekhar, V. C. J. *Am. Chem. Soc.* **1984**, *106*, 5034.
(15) Clucas, J. A.; Foster, D. F.; Harding, M. M.; Smith, A. K. *J. Chem. Soc., Chem. Commun.* **1984**, 949.
(16) Deeming, A. J.; Donovan-Mtunzi, S.; Kabir, S. E. *J. Organomet. Chem.* **1984**, *276*, C65.
(17) Deeming, A. J.; Donovan-Mtunzi, S.; Hardcastle, K. I.; Henrick, K.; McPartlin, M.; Kabir, S. E. *J. Chem. Soc., Dalton Trans.* **1988**, 579.
(18) Kabir, S. E.; Miah, A.; Nesa, L.; Uddin, K.; Hardcastle, K. I.; Rosenberg, E.; Deeming, A. J. *J. Organomet. Chem.* **1995**, *492*, 41.
(19) Watson, W. H.; Wu, G.; Richmond, M. G. *Organometallics* **2005**, *24*, 5431.
(20) Watson, W. H.; Wu, G.; Richmond, M. G. *Organometallics* **2006**, *25*, 930.
(21) Watson, W. H.; Poola, B.; Richmond, M. G. *J. Organomet. Chem.* **2006**, *691*, 4676.
(22) For recent examples, see: (a) Fairlamb, I. J. S.; Grant, S. McCormack, P.; Whittall, J. *Dalton Trans.* **2007**, 859. (b) Vavasori, A.; Bellieni, A.; Ronchin, L.; Acqua, F. D.; Toniolo, L.; Cavinato, G. *J. Mol. Catal. A: Chem.* **2007**, *263*, 9. (c) Ng, S. Y.; Leong, W. K. Goh, L. Y.; Webster, R. D. *Eur. J. Inorg. Chem.* **2007**, 463. (d) Ichikawa, H.; Ohno, Y.; Usami, Y.; Hrimoto, M. *Heterocycles* **2006**, *68*, 2247. (e) Cadierno, V.; Diez, J.; Garcia-Garrido, S. E.; Gimeno, J.; Nebra, N. *Adv. Synth Catal.* **2006**, *348*, 2125. (f) Wang, X. L.; Zheng, X. F.; Wang, L. Reiner, J.; Xie, W. L.; Chang, J. B. *Synthesis* **2007**, 989. (g) Wu, J.; Zhang, L.; Gao, K.; *Eur. J. Org. Chem.* **2006**, 5260.
(23) Brandoli, G.; Dolmella, A. *Coord. Chem. Rev.* **2000**, *209*, 161.
(24) Gan, K.-S.; Hor, T. S. A. In *Ferrocene*; Tongi, A., Hayashi T., Eds.; VCH: New York, 1995; Chapter 1.
(25) Colacot, T. J. *Platinum Met. Rev.* **2001**, 45.
(26) Yan, Y. K.; Chan, H. S. Q.; Hor, T. S. A.; Tan, K.-L.; Liu, L.-K.; Wen, Y.-S. *J. Chem. Soc., Dalton Trans.* **1992**, 423.
(27) Ohs, A. C.; Rheingold, A. L.; Shaw, M. J.; Nataro, C. *Organometallics* **2004**, *23*, 4655.
(28) Hor, T. S. A.; Phang, L.-T. *J. Organomet. Chem.* **1989**, *373*, 423.
(29) Hor, T. S. A.; Chan, H. S. O.; Tan, K.-L.; Phang, L.-T.; Yan, Y. K.; Liu, L.-K.; Wen, Y.-S. *Polyhedron* **1991**, *10*, 2437.
(30) Lu, X. L.; Ng, S. Y.; Vittal, J. J.; Tan, G. K.; Goh, L. Y.; Hor, T. S. A. *J. Organomet. Chem.* **2003**, *688*, 100.
(31) Kawano, H.; Nishimura, Y.; Onishi, M. *Dalton Trans.* **2003**, 1808.

Scheme 2

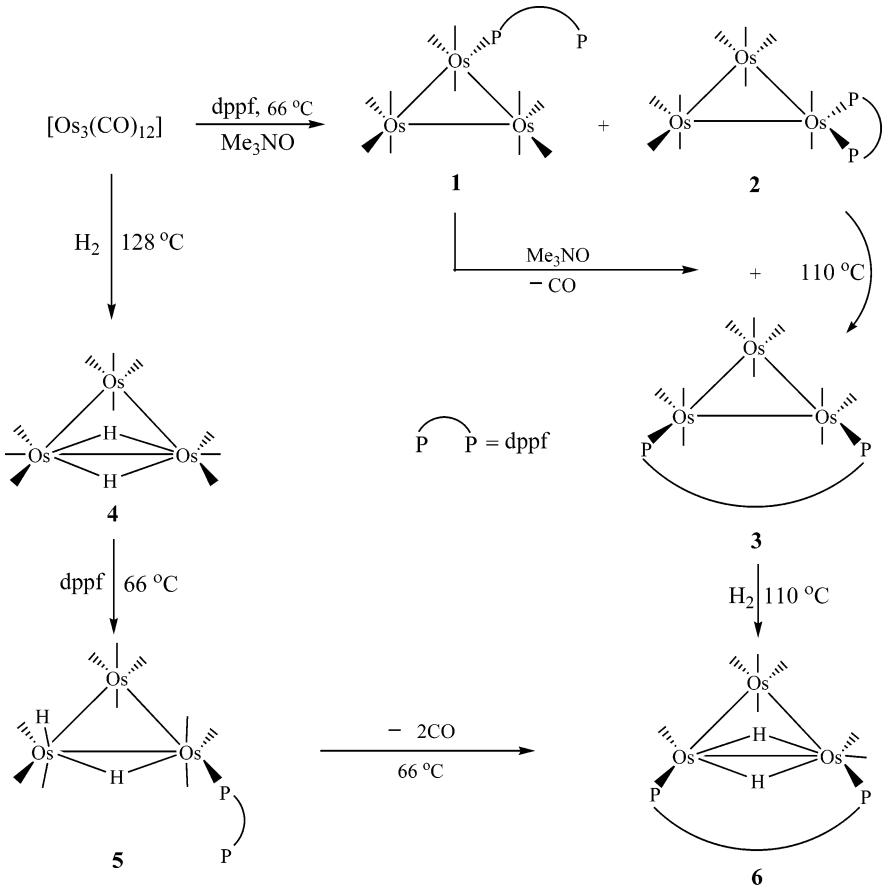

In comparison to the extensive number of trinuclear clusters, $[M_3(CO)_{10}(\text{diphosphine})]$ (M = Os, Ru), to date there have been only a few literature reports of trimetallic Group 8 carbonyls bearing the dppf ligand. Thus, three derivatives of $[Ru_3(CO)_{12}]$ containing dppf have been reported.[32,33] In two of these, $[Ru_3(CO)_{10}(\mu\text{-dppf})]$ and $[Ru_3(CO)_8(\mu\text{-dppf})_2]$, the dppf(s) bridge metal−metal bonds, whereas in $[\{Ru_3(CO)_{11}\}_2(\mu\text{-dppf})]$, it acts as open bridge, linking together the two triruthenium units. To our knowledge, the reactivity of dppf with simple triosmium clusters has not yet been investigated. In this report, we give details of the synthesis of a number of new triosmium and triruthenium dppf complexes, showing how the different coordination modes can be interconverted, and through a number of crystallographic studies, highlighting the ability of dppf to bridge a wide range of metal−metal distances.

Results and Discussion

Stepwise Conversion of Pendant to Chelate to Bridge dppf at the Triosmium Center: Crystal Structures of Bridge and Chelate Isomers. Heating equimolar amounts of $[Os_3(CO)_{12}]$ and dppf at 60 °C in the presence of Me_3NO leads to the complete consumption of the starting cluster in 1 h and furnishes three triosmium clusters: $[Os_3(CO)_{11}(\kappa^1\text{-dppf})]$ (**1**), $[Os_3(CO)_{10}(\kappa^2\text{-dppf})]$ (**2**), and $[Os_3(CO)_{10}(\mu\text{-dppf})]$ (**3**) in 10, 20, and 30% yields, respectively. Treatment of the labile cluster $[Os_3(CO)_{10}(MeCN)_2]$ with dppf at room temperature also affords **1**, **2**, and **3** in 5, 10, and 35% yields, respectively. Cluster **1** is a precursor of **2** and **3**, and we have shown in separate experiments that it converts into a mixture of **2** and **3** at room temperature via the Me_3NO initiated decarbonylation. Further, refluxing **2** in toluene cleanly affords **3**, confirming the reaction sequence **1** → **2** → **3**.

Since we were not able to obtain single crystals of **1**, its molecular structure was determined from spectroscopic data and elemental analysis. It is straightforwardly characterized by comparison with spectroscopic data of other pendant diphosphine clusters, $[Os_3(CO)_{11}(\kappa^1\text{-diphosphine})]$ (diphosphine = dppm, dppe, dppp).[39] The ν(CO) absorption spectrum is very similar to that observed for $[Os_3(CO)_{11}(\kappa^1\text{-dppe})]$, whereas the mass spectrum shows a molecular ion at *m*/*z* 1434 together with fragmentation peaks due to the sequential loss of all 11 CO ligands. In the room temperature ^{1}H NMR spectrum, in addition to aromatic protons, four equal intensity resonances at δ 4.43, 4.22, 4.12, and 3.90 (each integrating to 2H) are assigned to the protons of the cyclopentadienyl rings, whereas the $^{31}P\{^1H\}$ NMR spectrum displays two equal intensity singlets at δ −16.8 and 9.4, assigned to the free and coordinated diphenylphosphine groups, respectively.

The molecular structures of **2** and **3** can also be unambiguously assigned on the basis of spectroscopic data; for example,

(32) Chacon, S. T.; Cullen, W. R.; Bruce, M. I.; Shawkataly. O. B.; Einstein, F. W. B.; Jones, R. H.; Willis, A. C. *Can. J. Chem.* **1990**, *68*, 2001.
(33) O'Connor, A. R.; Nataro, C.; Rheingold, A. L. *J. Organomet. Chem.* **2003**, *679*, 72.
(34) Fabrizi de Biani, F.; Caudia, G.; Graiff, C.; Opromolla, G.; Predieri, G.; Tiripicchio, A.; Zanello, P. *J. Organomet. Chem.* **2001**, *637*−*639*, 586.
(35) Cauzzi, D.; Graiff, C.; Massera, C.; Predieri, G.; Tiripicchio, A.; Acquotti, D. *J. Chem. Soc., Dalton Trans.* **1999**, 3515.
(36) Cauzzi, D.; Graiff, C.; Lanfranchi, M.; Predieri, G.; Tiripicchio, A. *J. Organomet. Chem.* **1997**, *536*−*537*, 497.
(37) Kim, T.-J.; Kwon, S.-C.; Kim, Y.-H.; Heo, N. H.; Teeter, M. M.; Yamano, A. *J. Organomet. Chem.* **1991**, *426*, 71.
(38) Onaka, S.; Mizuno, A.; Takagi, S. *Chem. Lett.* **1989**, 2037.
(39) Deeming, A. J.; Donovan-Mtunzi, S.; Kabir, S. E. *J. Organomet. Chem.* **1987**, *333*, 253.

in their mass spectra, both exhibit a molecular ion peak at *m*/*z* 1406 corresponding to the formulation $[Os_3(CO)_{10}(dppf)]$ and fragment ions due to the sequential loss of 10 carbonyls. The pattern of ν(CO) absorption spectrum for **2** is similar to that of $[Os_3(CO)_{10}(\kappa^2\text{-dppe})]$[16] but quite different from isomeric **3**, indicating that the distribution of the carbonyl ligands differs between the two, whereas the ν(CO) absorption spectrum of **3** similarly bears a close resemblance to that of $[Os_3(CO)_{10}(\mu\text{-dppe})]$.[16,17] As usually found, these absorption frequencies are lower for the bridging isomer than for the corresponding chelating isomer. Both $^{31}P\{^1H\}$ NMR spectra show singlets, at δ −6.7 for **2** and at δ −5.0 for **3**, implying that both **2** and **3** contain equivalent phosphorus nuclei. These values should be compared to those of δ −6.4 and 37.4 for the bridge and chelate isomers of $[Os_3(CO)_{10}(dppv)]$, respectively.[19] Although chemical shifts for the bridge isomers are very similar, the small bite-angle of the diphosphine in $[Os_3(CO)_{10}(\kappa^2\text{-dppv})]$ leads to a marked downfield shift. The very similar values for **2** and **3** suggest that the phosphorus centers in these isomers have similar electronic properties. In the room temperature ^1H NMR spectra, **2** shows two signals at δ 4.52 and 4.37 and **3** exhibits a sharp signal at δ 4.57 and a broader one at δ 4.45 assigned to the cyclopentadienyl protons (In all these complexes, the ring protons should appear as virtual triplets. Generally, these were not resolved, and thus, we describe them as singlets or broad singlets.). Thus, spectroscopic data for **2** point to a structure with the dppf ligand chelating to a single osmium atom, whereas in **3** the dppf ligand is coordinated to two adjacent osmium atoms, and in both cases the phosphines occupy equatorial sites, i.e., in the plane of the osmium triangle.

To confirm this assertion and to compare the structures with those of the chelate and bridge isomers of $[Os_3(CO)_{10}(dppv)]$[19] and $[Os_3(CO)_{10}(dmpe)]$[40] reported by Richmond and Watson, we undertook X-ray crystallographic studies of both **2** and **3**. The molecular structure of **2** is shown in Figure 1 and, selected bond distances and angles are listed in the caption. The molecule consists of an isosceles triangle of osmium atoms with two longer but almost equal metal−metal bonds [Os(1)−Os(3) = 2.9241(2) Å and Os(1)−Os(2) = 2.9176(3) Å] and one relatively short metal−metal bond [Os(2)−Os(3) = 2.8859(2) Å] with 10 terminal carbonyl ligands, 4 bonded to Os(1) and 3 to each of Os(2) and Os(3). The average osmium−osmium distance of 2.9092(2) Å is in agreement with those in related triosmium clusters.[19−21,41] A salient feature of **2** is the coordination of the dppf ligand in a chelating mode to Os(1) and arranged equatorially so that the steric interaction between the phenyl rings and adjacent CO ligands is minimized. The Os−P bond distances [Os(1)−P(1) = 2.3425(10) Å and Os(2)−P(1) = 2.3284(10) Å] are comparable to those found in $[Os_3(CO)_{10}(\kappa^2\text{-dppv})]$ [2.299(2) and 2.293(2) Å].[19] The two longer Os−Os bonds are each *cis* to the dppf-chelated osmium atom, in agreement with previous observations that tertiary phosphine ligands tends to lengthen the *cis*-Os−Os bond in phosphine-substituted trimetallic clusters.[42] The two cyclopentadienyl ligands are staggered with respect to one another and the P(1)−Os(1)−P(2) bite angle of 105.89(4)° is consistent with *cis*-chelating dppf ligand and significantly larger than the analogous angles in $[Os_3(CO)_{10}(\kappa^2\text{-dppv})]$ [84.66(7)°],[16] $[Os_3(CO)_{10}(\kappa^2\text{-bpcd})]$ [87.15(6)°],[17] and $[Os_3(CO)_{10}(\kappa^2\text{-bmi})]$ [87.3(2)°].[18]

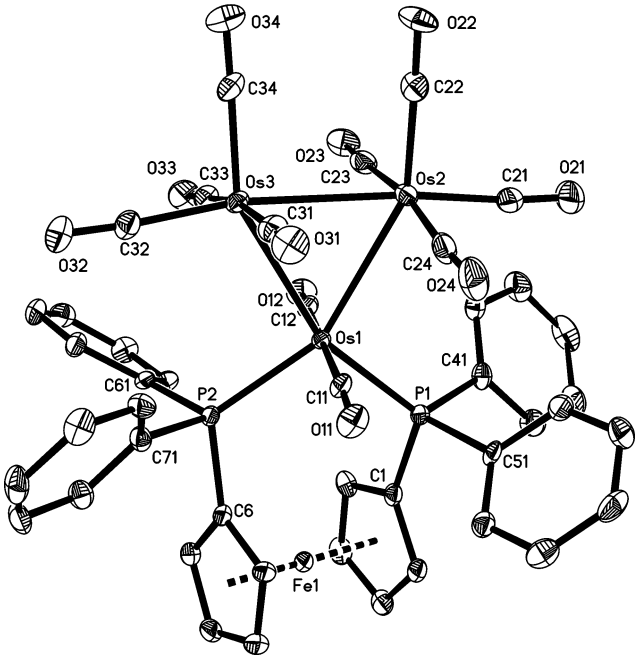

Figure 1. ORTEP diagram of $[Os_3(CO)_{10}(\kappa^2\text{-dppf})]$ (**2**) showing 50% probability thermal ellipsoids. Selected interatomic distances (Å) and angles (deg): Os(1)−Os(2) = 2.9176(3), Os(1)−Os(3) = 2.9241(2), Os(2)−Os(3) = 2.8859(2), Os(1)−P(1) = 2.343(1), Os(1)−P(2) = 2.328(1), Fe−C(av) = 2.0398(4), P(1)...P(2) = 3.73, P(2)−Os(1)−P(1) = 105.89(4), P(1)−Os(1)−Os(2) = 100.79(2), P(1)−Os(1)−Os(3) = 160.00(3), C(11)−Os(1)−Os(2) = 92.3(1), P(2)−Os(1)−Os(2) = 153.32.(3), P(2)−Os(1)−Os(3) = 94.11.-(3), C(12)−Os(1)−Os(3) = 93.4(1), C(12)−Os(1)−Os(2) = 90.73-(12), Os(2)−Os(2)−Os(1) = 60.28(1), Os(2)−Os(1)−Os(3) = 59.210(5), Os(3)−Os(2)−Os(1) = 60.507(6).

Reactions of $[Ru_3(CO)_{12}]$ with dppf yield only the bridging complex $[Ru_3(CO)_{10}(\mu\text{-dppf})]$[32] and to our knowledge, the chelating coordination mode of the dppf ligand on a trinuclear group 8 metal cluster has only previously been observed once before.[35] Thus, Predieri and co-workers have reported that reaction of the diselenide of dppf ($dppfSe_2$) with $[Ru_3(CO)_{12}]$ in the presence of Me_3NO affords the open triruthenium cluster $[Ru_3(CO)_7(\mu_3\text{-Se})_2(\kappa^2\text{-dppf})]$ in which the dppf ligand chelates to an open ruthenium atom. The bridge isomer is seen in small amounts and no attempt at converting one into the other was made. Interestingly, the dppe analogue, $[Ru_3(CO)_7(\mu_3\text{-Se})_2(\mu\text{-dppe})]$, exists only in the bridging form, highlighting the better chelating ability of dppf vs dppe.

The molecular structure of **3** is shown in Figure 2 and, selected bond distances and angles are listed in the caption. The three osmium atoms define an isosceles triangle with two short [Os(1)−Os(2) = 2.8816(3) Å, Os(2)−Os(1A) = 2.8816(3) Å] and one longer [Os(1)−Os(1A) = 2.9507(4) Å] osmium−osmium distances and of the 10 carbonyl ligands, 4 are bonded to Os(2) and 3 to each of Os(1)/Os(1A). The dppf ligand bridges the Os(1)−Os(1A) edge, occupying adjacent equatorial coordination sites the phosphine moieties lying trans to the non-bridged osmium−osmium edges [P(1)−Os(1)−Os(2) = 170.27-(3)°]. The dppf bridged vector [Os(1)−Os(1A) = 2.9507(4) Å] is significantly longer than the nonbridged osmium−osmium bonds, which is in contrast to the situation in $[Os_3(CO)_{10}(\mu\text{-dppe})]$ [2.891(1) vs 2.878(1), 2.871(1) Å][17] and $[Os_3(CO)_{10}(\mu\text{-dmpe})]$ [2.8832(6) vs 2.8819(6), 2.8817(6) Å].[40] The osmium−

(40) Watson, W. H.; Poola, B.; Richmond, M. G. *J. Chem. Crystallogr.* **2006**, *36*, 123.

(41) (a) Hansen, V. K.; Ma, A. K.; Biradha, R. K.; Pomeroy, R. K.; Zaworotko, *Organometallics* **1998**, *17*, 5267. (b) Bruce, M. I.; Liddell, M. J.; Hughes, C. A.; Patrick, J. M.; Skelton, B. W.; White, A. H. *J. Organomet. Chem.* **1988**, *347*, 157. (c) Kazemifar, N. K. K.; Stchedroff, M. J.; Mottalib, M. A.; Selva, S.; Monari, M.; Nordlander, E. Eur. J. *Inorg. Chem.* **2006**, 2058.

(42) Dierkes, P.; van Leeuwen, P. W. N. M. *J. Chem. Soc., Dalton Trans.* **1999**, 1519.

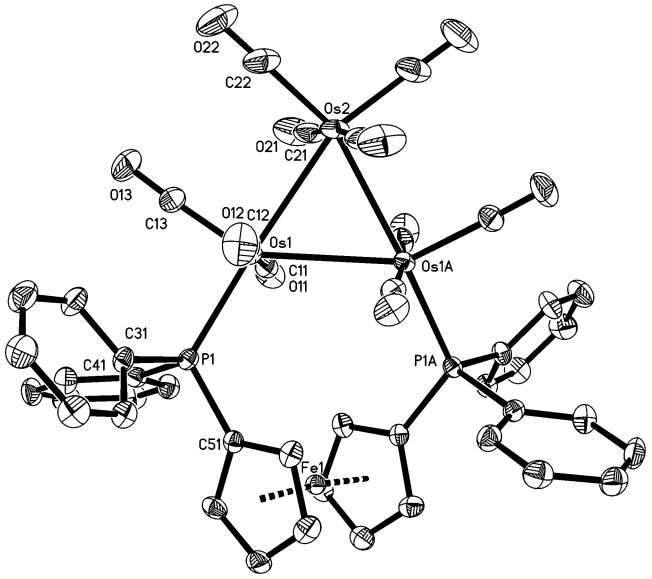

Figure 2. ORTEP diagram of $[Os_3(CO)_{10}(\mu\text{-dppf})]$ (**3**) showing 50% probability thermal ellipsoids. Selected interatomic distances (Å) and angles (deg): Os(1)−Os(2) = 2.8816(3), Os(1)−Os(1A) = 2.9507(4), Os(1)−P(1) = 2.349(1), Fe−C(av) = 2.042(1), P(1)...P(1A) = 5.20, P(1)−Os(1)−Os(2) = 170.27(3), C(11)−Os(1)−Os(2) = 95.3(1), C(11)−Os(1)−Os(1A) = 80.75(13), P(1)−Os(1)−Os(1A) = 117.82.(3), C(13)−Os(1)−Os(1A) = 147.0(1), Os(1)−Os(2)−Os(1A) = 61.594(9), C(12)−Os(1)−Os(2) = 84.08(14), C(12)−Os(1)−Os(1A) = 92.1(1), Os(2)−Os(2)−Os(1A) = 59.203(4).

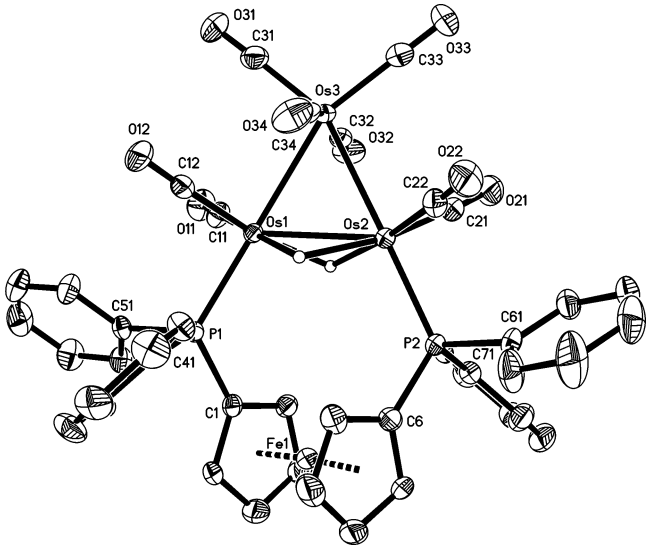

Figure 3. ORTEP diagram of $[Os_3(CO)_8(\mu\text{-dppf})(\mu\text{-H})_2]$ (**6**) showing 50% probability thermal ellipsoids. Selected interatomic distances (Å) and angles (deg): Os(1)−Os(2) = 2.7167(3), Os(2)−Os(3) = 2.8164(2), Os(2)−Os(3) = 2.8253(2), Os(1)−P(1) = 2.3327(9), Os(2)−P(2) = 2.3511(9), Fe−C(av) = 2.0411(4), P(1)−Os(1)−Os(2) = 116.74(2), P(2)−Os(2)−Os(1) = 117.68(3), P(1)−Os(1)−Os(3) = 172.16(2), P(2)−Os(2)−Os(3) = 176.84(3), C(11)−Os(1)−Os(2) = 127.1(1), C(12)−Os(1)−Os(2) = 129.7(1), C(21)−Os(2)−Os(1) = 128.3(1), C(22)−Os(2)−Os(1) = 127.8(1), Os(1)−Os(2)−Os(3) = 61.050(5), Os(2)−Os(1)−Os(3) = 61.378(6), Os(1)−Os(3)−Os(2) = 57.572(6).

phosphorus bond distances [Os(1)−P(1) = 2.3425(10) Å, Os(1)−P(2) = 2.3284(10) Å] are almost the same as those in **2** and $[Os_3(CO)_{10}(\mu\text{-dppe})]$ [2.328(3) and 2.333(3) Å].[17] A major difference between **2** and **3** is the relative conformations of the cyclopentadienyl rings. Whereas in **3** they are eclipsed (imposed by crystal symmetry), in **2** they are staggered. Coordination of dppf across the Os(1)−Os(1A) edge results in a significant stretching of the ligand relative to cluster **2**. The inter-nuclear P(1)−P(1A) distance of 5.20 Å found for **3** is some 1.47 Å longer than the corresponding P(1)−P(2) distance of 3.73 Å in **2**.

Upon heating in refluxing toluene, chelate **2** slowly converts to the bridge isomer **3**, a process which is irreversible. This observation is in contrast to those reported by Richmond and co-workers for the chelate-bridge pair $[Os_3(CO)_{10}(dppv)]$ in which isomerization is reversible[16] and $[Os_3(CO)_{10}(bpcd)]$[17] and $[Os_3(CO)_{10}(bmi)]$[18] in which irreversible bridge to chelate isomerization occurs. Further, we note that for $[Os_3(CO)_{10}(diphosphine)]$ (diphosphine = dppe, dppp), although both chelate and bridge isomers are accessible, no isomerization is observed. Our observations with dppe and dppp also parallel a recent report by Richmond et al.[40] on $[Os_3(CO)_{10}(dmpe)]$ where chelate-bridge isomerization is also absent. Hence, it is clear that the nature of the diphosphine plays a crucial role in chelate−bridge isomerization.

Synthesis and Crystal Structure of $[Os_3(CO)_8(\mu\text{-dppf})(\mu\text{-H})_2]$. Reactions of the unsaturated triosmium cluster $[Os_3(CO)_{10}(\mu\text{-H})_2]$ (**4**) with a range of diphosphines has been carried out. Significantly, in all cases, the bridge complexes $[Os_3(CO)_8(\mu\text{-diphosphine})(\mu\text{-H})_2]$ are the sole products of dicarbonyl substitution, with the diphosphine always bridging the short $Os(\mu\text{-H})_2Os$ edge.[43] Thus, recently we reported the chiral diphosphine substituted compounds $[Os_3(CO)_8(\mu\text{-diphosphine})(\mu\text{-H})_2]$ (diphosphine = BINAP, R-tol-BINAP and DIOP) from their thermal reactions with $[Os_3(CO)_{10}(\mu\text{-H})_2]$.[43] We were interested to see if a chelate complex of dppf could be prepared at this metal center and also wanted to prepare the bridge complex to compare its fluxionality with that of **3**. Hence, following our synthetic procedure, the addition of 1 equiv of dppf to a purple solution of **4** resulted in an immediate color change to yellow. Comparison of the IR spectrum with those of known adducts, $[HOs_3(CO)_{10}(L)(\mu\text{-H})]$,[43] indicated formation of $[HOs_3(CO)_{10}(\kappa^1\text{-dppf})(\mu\text{-H})]$ (**5**). This was not isolated, but heating the solution at 66 °C for 4 h led to the clean formation of $[Os_3(CO)_8(\mu\text{-dppf})(\mu\text{-H})_2]$ (**6**) (Scheme 1), isolated after chromatography as green crystals (64% yield). Cluster **6** was also obtained upon hydrogenation of **3**. It has been characterized by a combination of IR, ^{1}H NMR, and $^{31}P\{^1H\}$ NMR and single-crystal X-ray diffraction studies. The ν(CO) spectrum is very similar to that of $[Os_3(CO)_8(\mu\text{-BINAP})(\mu\text{-H})_2]$, suggesting that they are isostructural.[43] At room temperature, the hydride region of the ^{1}H NMR shows a triplet at δ −9.33 (J_{P-H} = 6.8 Hz) integrating to 2H, whereas the aliphatic region contains a sharp singlet at δ 4.39 and a broad singlet δ 3.94 each integrating for 4H. A singlet at δ −7.2 in the $^{31}P\{^1H\}$ NMR indicates equivalent ^{31}P nuclei. On the basis of this data, a bridging diphosphine was suggested, and to confirm this, an X-ray structure was undertaken.

The molecular structure of **6** is shown in Figure 3 and selected bond distances and angles are listed in the caption. The structure contains an isosceles triangle of osmium atoms, one bearing four carbonyl groups and the others two. The hydride ligands were crystallographically located and refined and found to bridge across the shortest Os(1)−Os(2) edge. The orientation of the equatorial carbonyl groups [C(11)−Os(1)−Os(2) = 127.08(13)°, C(12)−Os(1)−Os(2) = 129.71(13)°, C(21)−Os(2)−Os(1) =

(43) Stchedroff, M.; Moberg, V.; Rodriguez, E.; Aliev, A. E.; Bottcher, J.; Steed, J. W.; Nordlander, E.; Monari, M.; Deeming, A. J. *Inorg. Chim. Acta* **2006**, *359*, 926.

Scheme 3

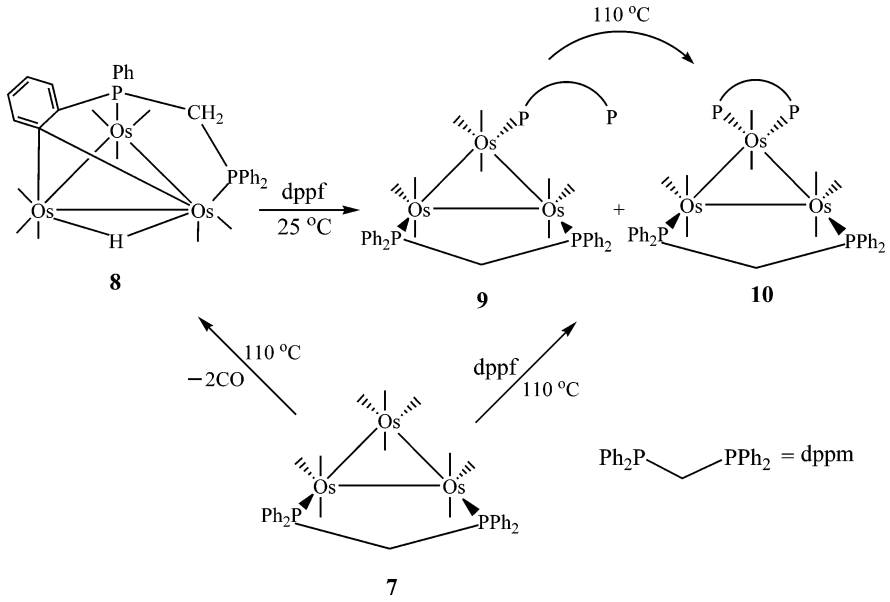

128.30(14)°, C(22)−Os(2)−Os(1) = 127.81(14)°], which are bent away from the this site, also supports this observation. The dppf ligand also bridges across the hydride-bridged vector, binding in equatorial sites. The osmium−osmium distance between bridged metal atoms [Os(1)−Os(2) = 2.7167(3) Å] is significantly shorter than the unbridged distances [Os(1)−Os(3) = 2.8164(2) Å, Os(2)−Os(3) = 2.8253(2) Å], being attributed to its formal double bond character. Cluster **6** closely resembles precursor **4**, whose structure was determined by both X-ray[44] and neutron diffraction[45] studies. The unbridged osmium−osmium distance is comparable with the Os═Os double bond distance of 2.681(1) Å in **4**.[44] The osmium−phosphorus bond distances [Os(1)−P(1) = 2.3327(9) Å, Os(2)−P(2) = 2.3511(9) Å] are comparable to the corresponding distances in $[Os_3(CO)_8(\mu\text{-dppm})(\mu\text{-H})_2]$, synthesized from the reaction of **8** with molecular hydrogen.[46] The Os−Os−P angles in the flexible dppf coordinated phosphametallacyclic ring in **6** [Os(1)−Os(2)−P(2) = 117.68(3)°, Os(2)−Os(1)−P(1) = 116.74(2)°] are significantly larger than the corresponding angles in $[Os_3(CO)_8(\mu\text{-dppm})(\mu\text{-H})_2]$ [95.3(1), 93.4(1)°],[46] implying that the ring size and strain of the phosphametallacycle exerts some influence on the geometry at the coordinated osmium centers. The cyclopentadienyl rings in **6** are eclipsed. Another effect of the short Os(1)−Os(2) edge is seen in the P...P separation of 4.88 Å, being shorter by 0.48 Å than the corresponding nonbonding separation in **3**. Formation of dihydride **6** from the ring-closure of **5** is in contrast to that observed for **1**, which furnishes both chelate and bridge isomers. The latter coordination is most probably favored over the chelate since in the bridging mode the metallacycle can alleviate the steric strain more efficiently than in a chelating mode.

Mixed Diphosphine Complexes. The Interplay Between Chelate and Bridge Coordination Modes. We were interested in preparing a triosmium cluster containing both dppm and dppf ligands to assess their relative propensity to adopt bridge or chelate coordination modes. The bridging capability of dppm is well-established.[13] This is highlighted in the structure of $[Os_3(CO)_8(\mu\text{-dppm})_2]$, formed upon addition of dppm to $[Os_3(CO)_{10}(\mu\text{-dppm})]$ (**7**) and in which both diphosphines adopt bridging modes *despite* this leading to one of them occupying the unfavorable axial coordination sites.[18] The unsaturated cluster $[Os_3(CO)_8\{\mu_3\text{-}Ph_2PCH_2P(Ph)C_6H_4\}(\mu\text{-H})]$ (**8**) acts as a source of dppm, reacting with monodentate phosphines at room temperature to give bis(adducts) $[Os_3(CO)_8(PR_3)_2(\mu_2\text{-dppm})]$ as the major products, together with small amounts of the monosubstituted orthometalated complexes $[Os_3(CO)_8(PR_3)\{\mu_3\text{-}Ph_2PCH_2P(Ph)C_6H_4\}(\mu\text{-H})]$. This then provides a useful low-temperature route to mixed phosphine derivatives of $[Os_3(CO)_{12}]$.[47] Thus, to synthesize dppf derivatives of **7** without resorting to extended thermolysis (which may result in secondary isomerization reactions), we investigated the reaction of **8** with dppf. Addition of dppf to **8** at room temperature leads to the formation of $[Os_3(CO)_9(\kappa^1\text{-dppf})(\mu\text{-dppm})]$ (**9**) and $[Os_3(CO)_8(\kappa^2\text{-dppf})(\mu\text{-dppm})]$ (**10**) (Scheme 3) in 33 and 44% yields, respectively. Unfortunately, we were unable to obtain X-ray quality crystals of either, but unequivocal characterization was made on the basis of analytical and spectroscopic data.

In **9**, the presence of a dangling dppf and a bridging dppm is easily deduced from the $^{31}P\{^1H\}$ NMR spectrum, which exhibits four equal intensity signals; a pair of doublets at δ −24.1 and −27.9 (J_{P-P} = 30 Hz) and two singlets at δ −16.5 and −9.1. The former are readily assigned to a bridging dppm ligand and the latter to the pendant dppf. The ^1H NMR spectrum shows four singlets in the aliphatic region at δ 4.39, 4.23, 4.15, and 3.83 due to the cyclopentadienyl protons and a triplet at δ 4.96 assigned to the methylene protons of the dppm ligand. As detailed for **1**, the presence of four cyclopentadienyl resonances is compatible with the pendant coordination of dppf. The FAB mass spectrum shows a molecular ion peak at *m*/*z* 1762 together with peaks due to the sequential loss of all nine carbonyls. Cluster **9** is isostructural with $[Os_3(CO)_9(\kappa^1\text{-dppm})(\mu\text{-dppm})]$, synthesized from the reaction of **7** with dppm and characterized by X-ray diffraction studies.[18] It formally results from simul-

(44) (a) Allen, V. F.; Mason, R.; Hitchcock, P. B. *J. Organomet. Chem.* **1977**, *140*, 297. (b) Churchill, M. R.; Hollander, F. J.; Hutchinson, J. P. *Inorg. Chem.* **1977**, *16*, 2697.

(45) Broach, R. W.; Williams, J. M. *Inorg. Chem.* **1979**, *18*, 314.

(46) Clucas, J. A.; Foster, D. F.; Harding, M. M.; Smith, A. K. *J. Chem. Soc., Chem. Commun.* **1985**, 2080.

(47) (a) Brown, M. P.; Dolby, P. A.; Harding, M. M.; Mathews, A. J. Smith, A. K.; *J. Chem. Soc., Dalton Trans.* **1993**, 1671. (b) Azam, K. A.; Hursthouse, M. B.; Islam, Md. R.; Kabir, S. E.; Malik, K. M. A.; Rashid, M. A.; Sudbrake, C.; Vahrenkamp, H. *J. Chem. Soc., Dalton Trans.* **1998**, 1097.

Scheme 4

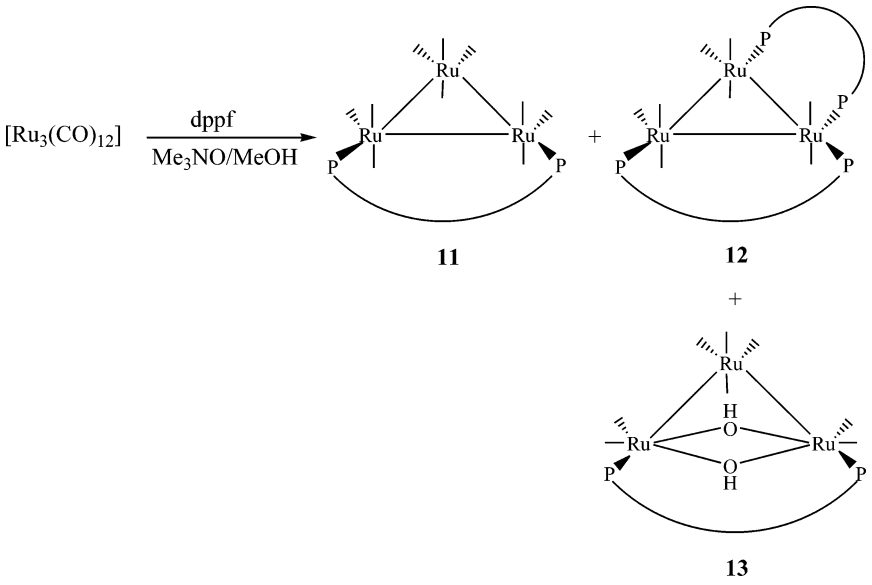

taneous addition of carbonyl and dppf ligands followed by reductive-elimination of the orthometalated phenyl group of the diphosphine.

The ν(CO) pattern of **10** is quite different from that of $[Os_3(CO)_8(\mu\text{-dppm})_2]$, which was synthesized from the reaction of **7** with dppm at 110 °C, indicating that they have different distribution of carbonyl ligands.[18] The $^{31}P\{^1H\}$ NMR spectrum is very simple, showing only two equal intensity singlets at δ −32.5 and −7.5 and suggesting that dppm is bound to two adjacent metal atoms in an edge-bridging mode and the dppf chelates to the third metal. Apart from the multiplets in the aromatic of the ^1H NMR spectrum, in the aliphatic region, a triplet at δ 4.87 is assigned to the equivalent methylene protons of the dppm and two singlets at δ 4.52 and 4.31 are assigned to the cyclopentadienyl protons of the dppf. The FAB mass spectrum exhibits a molecular ion peak at *m*/*z* 1734 corresponding to $[Os_3(CO)_8(dppf)(dppm)]$ and fragmentation peaks due to the successive loss of eight carbonyls.

Spectroscopic data for **10** clearly point toward a structure in which the dppf is chelating (in equatorial sites) to one osmium atom while the dppf bridges the other two metal atoms again occupying equatorial sites. Alternative structures with both dppm and dppf ligands in edge-bridging coordination modes can be ruled out on the basis of ^{31}P NMR data and although a second conformation in which the dppf is bridging and the dppm chelating cannot be unequivocally dismissed, the strong bridging propensity of dppm and its position in this site in the starting material point clearly to the proposed molecular structure. This is further supported by the clean conversion of **9** (with a bridging dppm) to **10** upon heating at 110 °C in toluene. The chelating mode of the dppf in **10** is probably favored since it can alleviate the steric strain of the diphosphine more efficiently than if it bridges to the other metal.

Reactions of Triruthenium Clusters with dppf: Bridging of Dihydroxy and dppf Across Open Ruthenium−Ruthenium Edge. Reactions between $[Ru_3(CO)_{12}]$ and dppf have previously been explored under a variety of different conditions leading to the formation of $[Ru_3(CO)_{10}(\mu\text{-dppf})]$ (**11**), $[Ru_3(CO)_8(\mu\text{-dppf})_2]$ (**12**), and the linked hexanuclear cluster $[\{Ru_3(CO)_{11}\}_2(\mu\text{-}\kappa^1,\kappa^1\text{-dppf})]$.[32,33] In no instance is a chelate dppf complex identified. More generally, $[Ru_3(CO)_{12}]$ has been shown to react with diphosphines in the presence of Me_3NO to give substituted derivatives.[48] Since we were interested in the possibility of forming a pendant dppf complex and perhaps even a chelate derivative, we carried out the reaction of $[Ru_3(CO)_{12}]$ and dppf using Me_3NO as an activating agent. Somewhat surprisingly then we found that the reaction of $[Ru_3(CO)_{12}]$ with dppf in the presence of Me_3NO gave, in addition to the previously reported[32] clusters **11** and **12**, the dihydroxy compound $[Ru_3(CO)_8(\mu\text{-dppf})(\mu\text{-OH})_2]$ (**13**) as the major product (Scheme 4). To investigate the formation of **13** more fully, we found that addition of a drop of water to the reaction mixture increased the yield of **13** up to 40%. Thus, we believe that the origin of the hydroxy ligands in **13** is most probably water. Cluster **11** was previously reported by Bruce et al.[33] to be formed in 76% yield from the [PPN][acetate] catalyzed reaction of $[Ru_3(CO)_{12}]$ with dppf and **12** by a thermal reaction at 80 °C. To see if the dihydroxide **13** was also formed in the ketyl catalyzed reaction, we investigated the reaction of $[Ru_3(CO)_{12}]$ with dppf in the presence of sodium diphenylketyl and obtained **11** as the only product (85% yield). This is in contrast to the report of Bruce and co-workers who obtained a very-low yield of **11** from the sodium diphenylketyl catalyzed reaction.[32]

The new cluster **13** was characterized by spectroscopic data and unequivocally by an X-ray diffraction study. In addition to the phenyl proton resonances in the aromatic region, the ^1H NMR spectrum shows two multiplets at δ 4.80 and 4.22 assigned to the cyclopentadienyl protons and a triplet at δ −0.68 (J_{P-H} = 3.4 Hz) due to the hydroxide bridges. The latter is typical and compares well with that of other structurally characterized hydroxyl-bridged trimetallic complexes: $[Ru_3(CO)_8(\mu\text{-BINAP})(\mu\text{-OH})_2]$ [δ −1.48, J_{P-H} = 4.0 Hz],[48] $[Os_3(CO)_8(\mu\text{-dppm})(\mu\text{-OH})(\mu\text{-H})]$ [δ −0.44, J_{P-H} = 4.3 Hz],[49] and $[Os_3(CO)_8(PPh_3)_2(\mu\text{-OH})_2(\mu\text{-H})]$ [δ −0.18, J_{P-H} = 3.6 Hz].[50] The $^{31}P\{^1H\}$ NMR spectrum shows a singlet at δ 2.4, indicating the equivalence of the phosphorus atoms. The ν(CO) region of the IR spectrum is very similar to that of $[Ru_3(CO)_8(\mu\text{-BINAP})(\mu\text{-OH})_2]$, suggesting they are isostructural.[48]

(48) Deeming, A. J.; Speel, D. M.; Stchedroff, M. *Organometallics* **1997**, *16*, 6004.

(49) Hodge, S. R.; Johnson, B. F. G.; Lewis, J.; Raithby, P. R.; *J. Chem. Soc., Dalton Trans.* **1987**, 931.

(50) Akter, H.; Deeming, A. J.; Hossain, G. M. G.; Kabir, S. E.; Mondol, D. N.; Nordlander, E.; Sharmin, A.; Tocher, D. A. *J. Organomet. Chem.* **2005**, *690*, 4639.

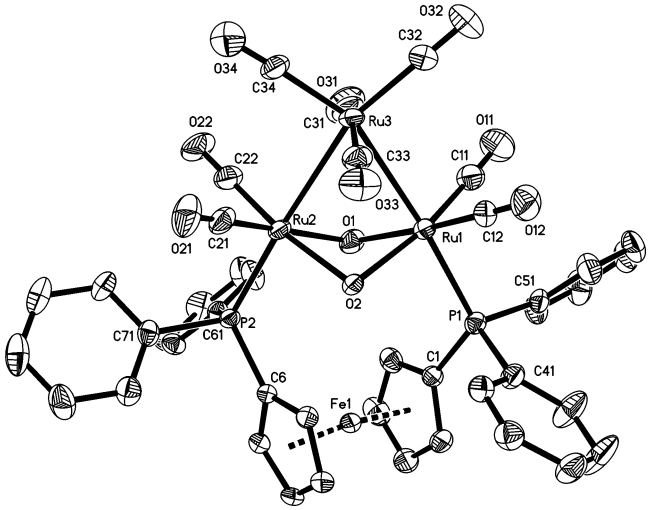

Figure 4. ORTEP diagram of $[Ru_3(CO)_8(\mu\text{-dppf})(\mu\text{-OH})_2]$ (**13**) showing 50% probability thermal ellipsoids. Selected interatomic distances (Å) and angles (deg): Ru(1)−Ru(3) = 2.8345(5), Ru(1)−Ru(3) = 2.8317(6), Ru(1)...Ru(2) = 3.0308(6), Ru(1)−O(1) = 2.111(3), Ru(2)−O(1) = 2.119(4), Ru(1)−O(2) = 2.128(3), Ru(2)−O(2) = 2.135(3), Fe−C(av) = 2.042(6), Ru(1)−P(1) = 2.391(1), Ru(2)−P(2) = 2.365(1), P(1)...P(2) = 5.26, O(1)−Ru(1)−Ru(3) = 83.7(1), O(2)−Ru(1)−Ru(3) = 85.85(9), P(1)−Ru(1)−Ru(3) = 175.16(3), P(2)−Ru(2)−Ru(3) = 172.41(3), O(1)−Ru(1)−O(2) = 75.4(1), O(1)−Ru(2)-O(2) = 75.1(1), O(2)−Ru(2)−Ru(3) = 85.80(9), O(1)−Ru(2)−Ru(3) = 83.7(1), Ru(2)−Ru(3)−Ru(1) = 64.67(1), Ru(1)−O(1)−Ru(2) = 91.5(1), Ru(1)−O(2)−Ru(2) = 90.7(1).

To confirm this, the molecular structure of **13** was determined the results of which are shown in Figure 4 and selected bond distances and angles are listed in the caption. The molecule consists of an open cluster of three ruthenium atoms with two equal metal−metal bonds [Ru(2)−Ru(3) = 2.8317(6) Å and Ru(1)−Ru(3) = 2.8345(5) Å], eight terminal carbonyl groups, two bridging hydroxyl ligands, and a bridging dppf ligand. The nonbonded Ru(1)....Ru(2) distance of 3.0308(6) Å is significantly longer than the two bonded ruthenium−ruthenium distances but, interestingly, it is still within the accepted range of ruthenium−ruthenium bonding distances.[51] Nevertheless, the cluster is electron-precise without the Ru(1)−Ru(2) bond. It is possible that unusual shortening of the nonbonded vector is due to the presence of the two hydroxyl-bridges, and in support of this, we note that a similar shortening is seen in $[Ru_3(CO)_8(\mu\text{-BINAP})(\mu\text{-OH})_2]$ [3.023(2) Å].[48] Interestingly, the bridging dppf ligand in $[Ru_3(CO)_7(\mu\text{-dppf})(\mu^3\text{-Se})_2]$ spans the nonbonded ruthenium−ruthenium edge [Ru...Ru = 3.83 Å],[34] which is significantly longer than that observed in **13**. Therefore, it is likely this distance in **13** is controlled by hydroxyl-bridges and not by the dppf itself. Both hydroxide groups are symmetrically bound, the ruthenium−oxygen distances [Ru(1)−O(1) = 2.111(3) Å, Ru(2)−O(1) = 2.119(3) Å, Ru(1)−O(2) = 2.128(3) Å, Ru(2)−O(2) = 2.135(3) Å] being comparable to those in $[Ru_3(CO)_8(\mu\text{-BINAP})(\mu\text{-OH})_2]$ [2.118(13)−2.102(13) Å].[48] As expected, the phosphorus atoms of the dppf ligand occupy equatorial sites and the two ruthenium−phosphorus distances are unsymmetrical and somewhat longer [Ru(1)−(P(1) = 2.3914(12) Å and Ru(2)−(P(2) = 2.3614(12) Å] than the corresponding distances in $[Ru_3(CO)_{10}(\mu\text{-dppf})]$ (**11**) [2.3503(8) Å].[32] The overall structure of **13** is similar to that of the BINAP analog $[Ru_3(CO)_8(\mu\text{-BINAP})(\mu\text{-OH})_2]$.[48]

(51) Adams, R. D.; Captain, B.; Fu, W.; Hall, M. B.; Smith, M. D.; Webster, C. D. *Inorg. Chem.* **2004**, *43*, 3921.

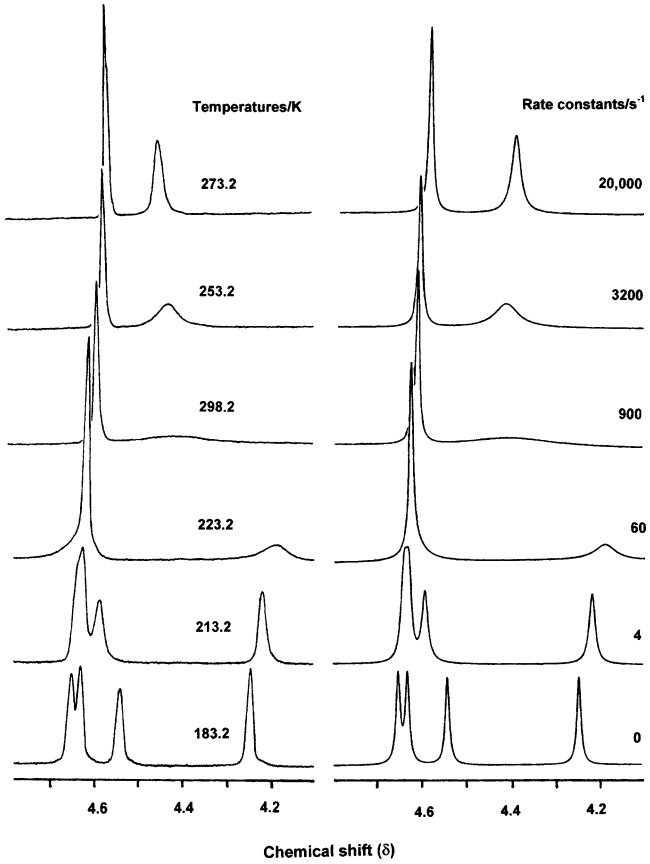

Figure 5. Observed (left) and computed (using gNMR[52]) (right) ^{1}H NMR spectra for $[Os_3(CO)_{10}(\mu\text{-dppf})]$ (**3**) measured in CD_2Cl_2 at 400 MHz.

Dynamic Behavior of dppf Complexes. As detailed in the introduction, dppf displays great conformational flexibility, which results from the tilting motion of the two cyclopentadienyl ring planes and a torsional rotation around the axis passing through the two ring centroids. In light of this, many dppf complexes are fluxional, being attributed to the mutual twisting of the cyclopentadienyl ligands and bridge-reversal at the metal.[30,35] The fluxionality of the dppf ligand in the trimetallic clusters $[Os_3(CO)_{10}(\kappa^2\text{-dppf})]$ (**2**), $[Os_3(CO)_{10}(\mu\text{-dppf})]$ (**3**), $[Os_3(CO)_8(\mu\text{-dppf})(\mu\text{-H})_2]$ (**6**), and $[Ru_3(CO)_8(\mu\text{-dppf})(\mu\text{-OH})_2]$ (**13**) were investigated in a series of variable-temperature ^{1}H NMR studies, monitoring changes to the cyclopentadienyl resonances. In chelate **2**, these appear as two pseudo-triplets at δ 4.52 and 4.37 at room temperature, suggesting that the two cyclopentadienyl ligands are twisting rapidly. Cooling a CD_2Cl_2 solution down to −90 °C resulted in little change, and importantly, the line width of the signals was virtually unchanged, suggesting that the twisting motion has a low activation energy when the ligand binds in a chelate manner. The room temperature ^{1}H NMR spectrum in CD_2Cl_2 of the bridge isomer **3** shows one sharp pseudo triplet (δ 4.57) and one broad signal (δ 4.45) assigned to the cyclopentadienyl protons but this changes significantly upon lowering the temperature (Figure 5a). Upon cooling to −30 °C, the latter broadens into the baseline, whereas the former remains quite sharp. By −70 °C, the upfield signal is resolved into a pair of singlets at δ 4.59 and 4.22, whereas the low-field signal now begins to split such that by −90 °C, four well-defined signals are apparent, those at δ 4.65 and 4.63 being attributed to the initial low-field signal. From these data, it is easy to measure the coalescence temperature of the upfield signal (ca. −30 °C) and thus extrapolate a free energy of activation ($\Delta G^{\#}$) of 47.4 ± 1.0 kJ mol^{-1} for the process. To

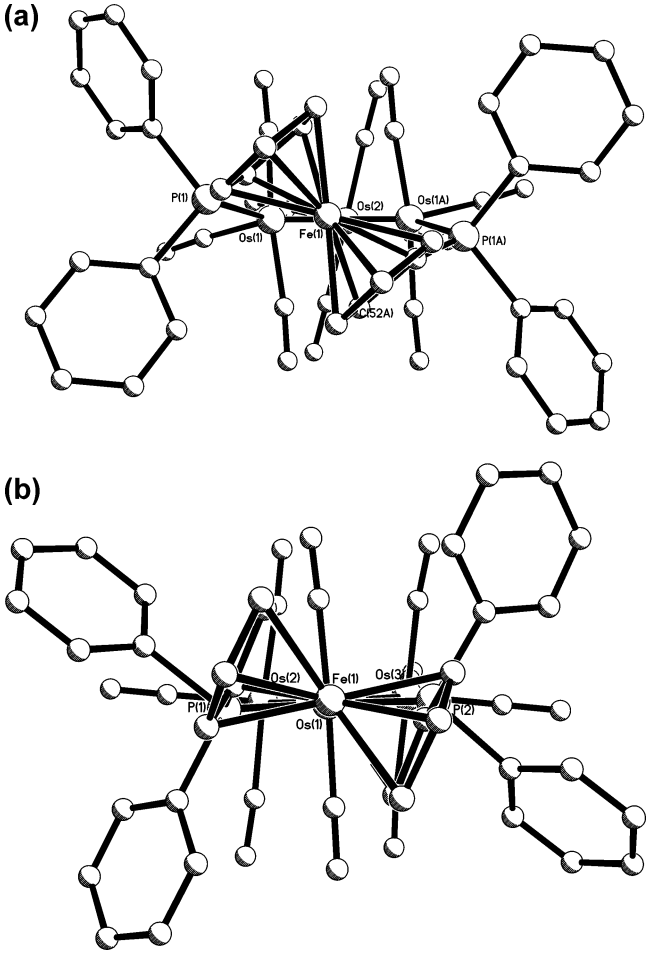

Figure 6. Views of (a) **3** and (b) **2** highlighting the orientation of the ferrocene unit of the dppf ligand with respect to the triosmium framework.

probe the thermodynamic parameters in more detail, the spectra were simulated using gNMR[52] (Figure 5b). From this analysis, values of 39.7 ± 1.0 kJ mol^{-1} and −30 ± 4 J K mol^{-1} were calculated for $\Delta H^{\#}$ and $\Delta S^{\#}$, respectively, giving a $\Delta G^{\#}$(298 K) of 48.6 ± 1.0 kJ mol^{-1}.

These observed changes are attributed to a torsional rotation around the axis passing through the two ring centroids which results in the twisting of the dppf ligand with respect to the plane of the triosmium triangle. This is illustrated in Figure 6, which shows views of **2** and **3** looking approximately parallel to the triosmium plane. For bridge isomer **3**, it is clear that this is greater than for chelate **2**, and this can be quantified by considering the angles between the plane of the three osmium atoms and that containing the iron atom and centroids of the cyclopentadienyl rings. Thus, in **2** the twisting is approximately 27.2°, whereas in **3** it is nearly twice as large at 49.6°. This difference probably accounts for the lower activation barrier for the process in **2** as compared to **3**. A similar torsional rotation was found in chelate [$Ru_3(CO)_7(\mu_3\text{-}Se)_2(\kappa^2\text{-dppf})$], although here, because of the inequivalence of the phosphine coordination sites, eight signals were observed at the low-temperature, and four at the high-temperature, limit.[35] A free energy of activation of 50.2 kJ mol^{-1} was measured, being considerably higher than that in **2**. This may be a result of the smaller bite-angle of the dppf ligand in [$Ru_3(CO)_7(\mu_3\text{-}Se)_2(\kappa^2\text{-dppf})$] [P−Ru−P 100.6(1)°] versus that of 105.89(4)° in **2**. We also note that this fluxional process is somewhat similar to the previously observed inversion of the OsPCCPOs ring in [$Os_3(CO)_{10}(\mu\text{-dppe})$].[17]

Variable-temperature ^{1}H NMR spectra of **6** show very similar changes to those discussed above for **3**. Thus, low-temperature limiting spectra consist of four well-separated signals (δ 4.77, 4.38, 4.02, 3.33), whereas at room temperature one sharp and one broad signal are observed. From an analysis of these data, thermodynamic parameters can be ascertained [$\Delta G^{\#}$(298 K) 43.6 ± 1.0 kJ mol^{-1}; $\Delta H^{\#}$ 32.0 ± 0.3 kJ mol^{-1}; $\Delta S^{\#}$ −39 ± 4 J K^{-1} mol^{-1}]. The free energy of activation is somewhat smaller than that measured for **3** ($\Delta\Delta G^{\#}$(298 K) ca. 5.0 kJ mol^{-1}), perhaps being a measure of the smaller degree of twisting seen in **6** (42.6°). Variable-temperature ^{1}H NMR spectra of **13** (twist angle 37.6°) follow a similar pattern to those discussed above, the major difference being the greater chemical shift range of the low-temperature limiting signals (δ 5.75, 4.39, 4.00, 3.58). Again, from a simulation of the spectra thermodynamic parameters could be extrapolated [$\Delta G^{\#}$(298 K) 44.2 ± 1.0 kJ mol^{-1}; $\Delta H^{\#}$ 34.4 ± 0.3 kJ mol^{-1}; $\Delta S^{\#}$ −33 ± 1 J K^{-1} mol^{-1}], the free energy of activation being similar to that measured in **6**. The latter is interesting since in the two clusters the dppf ligand spans quite different length metal−metal vectors [**6**, Os−Os = 2.7167(3) Å; **13**, Ru−Ru 3.0308(6) Å].

Conclusions

The present study has demonstrated that three coordination modes of dppf ligand are possible on trimetallic clusters: the thermally induced Me_3NO initiated reaction of [$Os_3(CO)_{12}$] with dppf providing sequentially [$Os_3(CO)_{11}(\kappa^1\text{-dppf})$] (**1**), [$Os_3(CO)_{10}(\kappa^2\text{-dppf})$] (**2**), and [$Os_3(CO)_{10}(\mu\text{-dppf})$] (**3**), although the bridging mode is the thermodynamic product. This contrasts with the reaction with [$Os_3(CO)_{10}(\mu\text{-H})_2$] (**4**) where the bridged complex [$Os_3(CO)_8(\mu\text{-dppf})(\mu\text{-H})_2$] (**6**) results and with saturated [$Os_3(CO)_{10}(\mu\text{-dppm})$] (**7**) or electron-deficient [$Os_3(CO)_8\{\mu_3\text{-}Ph_2PCH_2P(Ph)C_6H_4\}(\mu\text{-H})$] (**8**), which afford chelate [$Os_3(CO)_8(\mu\text{-dppm})(\kappa^2\text{-dppf})$] (**10**) as the final product, although both proceed via a pendant intermediate. The observation of chelating dppf and bridging dppm ligands in the latter suggests that dppf is the better chelating ligand of the two. Another finding of this study is the wide range of metal−metal bond distances that the dppf ligand can bridge across, accommodating these by varying the twist angle with respect to the trimetal framework. The fluxionality of a number of these clusters has been studied by VT NMR establishing the low-energy torsional rotation about metal-ring centroid vector and once again highlighting the tremendous flexibility of this ligand when bound to multinuclear metal centers.

Experimental Section

General Comments. Unless otherwise stated, all of the reactions were performed under a nitrogen atmosphere using standard Schlenk techniques. Solvents were dried and distilled prior to use by standard methods. [$Os_3(CO)_{12}$] and [$Ru_3(CO)_{12}$] were purchased from Strem Chemicals and 1,1′-*bis*(diphenylphosphino)ferrocene (dppf) was purchased from Aldrich and used as received. The compounds [$Os_3(CO)_{10}(\mu\text{-dppm})$],[15] [$Os_3(CO)_8\{\mu_3\text{-}Ph_2PCH_2P(Ph)C_6H_4\}(\mu\text{-H})$],[15] and [$Os_3(CO)_{10}(\mu\text{-H})_2$][53] were prepared according to published procedures. Infrared spectra were recorded on a Shimadzu FTIR 8101 spectrophotometer. ^{1}H and ^{31}P{^{1}H} NMR spectra were recorded on Varian Unity Plus 500 and Bruker DPX 400 instruments. All chemical shifts are reported in δ units with reference to

(52) *gNMR*, Ver. 4.1; Charwell Scientific Ltd.: Oxford, UK, 1995.

(53) Kaesz, H. D. *Inorg. Synth.* **1989**, *28*, 238.

Table 1. Crystallographic Data and Structure Refinement[a] for 2, 3, 6, and 13

	2	**3**·2CH_2Cl_2	**6**·1/2C_6H_{14}	**13**
Formula	$C_{44}H_{28}FeO_{10}Os_3P_2$	$C_{46}H_{32}Cl_4FeO_{10}Os_3P_2$	$C_{45}H_{37}FeO_8Os_3P_2$	$C_{42}H_{30}FeO_{10}P_2Ru_3$
M_w	1405.05	1574.91	1394.14	1115.66
cryst syst	orthorhombic	orthorhombic	monoclinic	monoclinic,
space group	$P2_1/c$	$Pbcn$	$P2_1/n$	$P2_1/n$
a (Å)	12.9196 (7)	16.3658 (9)	19.671(1)	19.920(1)
b (Å)	15.5471 (9)	16.2298 (9)	11.8123(7)	11.6063(8)
c (Å)	19.998 (1)	18.042 (1)	21.007(1)	21.438(2)
α (deg)	90	90	90	90
β (deg)	90	90	05.971(1)	108.091(1)
γ (deg)	90	90	90	90
V (Å$^{3)}$	4017.0 (4)	4792.3 (5)	4692.7(5)	4711.2(6)
Z	4	4	4	4
ρ (g cm^{-3})	2.323	2.183	1.973	1.573
μ (mm^{-1})	9.954	8.572	8.516	1.363
F(000)	2624	2960	2620	2200
size (mm^3)	0.49 × 0.30 × 0.21	0.44 × 0.36 × 0.26	0.45 × 0.24 × 0.05	0.28 × 0.16 × 0.12
θ_{max} (deg)	1.66 to 28.29	1.77 to 28.30	1.67 to 28.29	1.68 to 28.31
index ranges	$-17 \le h \le 16$	$-21 \le h \le 21$	$-26 \le h \le 26$	$-26 \le h \le 26$
	$-20 \le k \le 20$	$-21 \le k \le 21$	$-15 \le k \le 15$	$-15 \le k \le 15$
	$-26 \le l \le 25$	$-23 \le l \le 23$	$-27 \le l \le 28$	$-26 \le l \le 27$
reflns collected	35449	40419	39840	40988
independent reflns	9661 [R(int) = 0.0317]	5852 [R(int) = 0.0405]	11178 (R_{int} = 0.0412)	11256 (R_{int} = 0.0351)
reflections with $F^2 > 2\sigma$	9525	5479	10032	9867
$T_{max,}$ T_{min}	0.0847 and 0.2290	0.1165 and 0.2140	0.6754 and 0.1142	0.8535 and 0.7014
weighting parameters a, b	0.0044, 0.1138	0.0279, 27.1726	0.0336, 7.4150	0.0806, 13.3192
data/restraints/parameters	9661/0/541	5852/0/299	11178/0/567	11256/0/519
GOF on F^2	1.082	1.013	1.013	1.113
Final R indices [$I > 2\sigma(I)$]	R_1 = 0.0194	R_1 = 0.0296	R_1 = 0.0278	R_1 = 0.0546
	wR_2 = 0.0424	wR_2 = 0.0666	wR_2 = 0.0704	wR_2 = 0.1503
R indices (all data)	R_1 = 0.0199	R_1 = 0.0327	R_1 = 0.0323	R_1 = 0.0632
	wR_2 = 0.0426	wR_2 = 0.0683	wR_2 = 0.0725	wR_2 = 0.1558
largest diff peak and hole, e.Å^{-3}	1.538 and −0.773	1.245 and −1.043	1.854 and −0.929	2.066 and −0.909

[a] Details in common: X-radiation, Mo Kα (λ = 0.71073 Å), temperature (K) 150(2), refinement method: full-matrix least-squares on F^2.

the residual protons of the deuterated solvents for proton and to external 85% H_3PO_4 for ^{31}P chemical shifts. Elemental analyses were performed by the Microanalytical Laboratories, University College London. Fast atom bombardment mass spectra were obtained on a JEOL SX-102 spectrometer using 3-nitrobenzyl alcohol as matrix and CsI as calibrant.

Reaction of [Os$_3$(CO)$_{12}$] with dppf. A benzene (50 mL) suspension of [$Os_3(CO)_{12}$] (250 mg, 0.260 mmol) and dppf (152 mg, 0.274 mmol) was warmed to 60 °C for 1 h, and a solution of freshly sublimed Me_3NO (42 mg, 0.559 mmol) in MeOH (7 mL) was added dropwise from a pressure-equalizing dropping funnel (30 min), during which time the color changed from yellow to red. The solvent was removed under reduced pressure, and the residue was chromatographed by TLC on silica gel. Elution with hexane/CH_2Cl_2 (8:2, v/v) gave three bands. The faster-moving band afforded [$Os_3(CO)_{11}(\kappa^1$-dppf)] (**1**) (39 mg, 10%) as orange crystals after recrystallization from hexane/CH_2Cl_2 at −4 °C. Anal. calcd for $C_{45}H_{28}FeO_{11}Os_3P_2$: C, 37.71; H, 1.97. Found: C, 37.97; H, 2.15%. IR (ν(CO), CH_2Cl_2): 2107 s, 2054 vs, 2033 m, 2018 s, 1987 m, 1910 w cm^{-1}. ^{1}H NMR (CD_2Cl_2): δ 7.52 (m, 10H), 7.27 (m, 10H), 4.43 (s, 2H), 4.22 (s, 2H), 4.12 (s, 2H), 3.90 (s, 2H). ^{31}P-{^{1}H} NMR (CD_2Cl_2): δ −9.4 (s, 1P), −16.8 (s, 1P). FAB MS: m/z 1434 (M$^+$). The second band yielded [$Os_3(CO)_{10}(\kappa^2$-dppf)] (**2**) (68 mg, 20%) as orange crystals from hexane/CH_2Cl_2 at −4 °C. Anal. calcd for $C_{44}H_{28}FeO_{10}Os_3P_2$: C, 37.61; H, 2.01. Found: C, 37.8 4; H, 2.16%. IR (ν(CO), CH_2Cl_2): 2093 s, 2043 vs, 2006 vs, 1989 w, 1962 m, 1910 m cm^{-1}. ^{1}H NMR ($CDCl_3$): δ 7.63 (m, 10H), 7.33 (m, 10H), 4.52 (s, br, 4H), 4.37 (s, br, 4H). ^{31}P-{^{1}H} NMR ($CDCl_3$): δ −6.7 (s). FAB MS: m/z 1406 (M$^+$). The third band afforded [$Os_3(CO)_{10}(\mu$-dppf)] (**3**) (102 mg, 30%) as red crystals after recrystallization from hexane/CH_2Cl_2 at −4 °C. Anal. calcd for $C_{44}H_{28}FeO_{10}Os_3P_2$: C, 37.61; H, 2.01. Found: C, 37.78; H, 2.15%. IR (ν(CO), CH_2Cl_2): 2087 s, 2054 w, 2022 m, 2002 vs, 1968 w, 1952 w cm^{-1}. ^{1}H NMR (CD_2Cl_2): δ 7.58 (m, 10H), 7.43 (m, 10H), 4.57 (s, br, 4H), 4.45 (s, br, 4H). ^{31}P-{^{1}H} NMR (CD_2Cl_2): δ −5.0 (s). FAB MS: m/z 1406 (M$^+$).

Conversion of 1 to 2 and 3. To a dichloromethane solution (15 mL) of **1** (25 mg, 0.017 mmol) was added Me_3NO (2 mg, 0.027 mmol) and it allowed to stir for 1 h under a slow purge of N_2. The solvent was removed under reduced pressure, and the residue was taken up in CH_2Cl_2 and applied to silica ge TLC plates. Elution with hexane/CH_2Cl_2 (4:1, v/v) developed two bands. The faster-moving band afforded compound **2** (10 mg, 40%) and the slower-moving band gave **3** (8 mg, 32%).

Conversion of 2 to 3. A toluene solution (15 mL) of **2** (25 mg, 0.018 mmol) was refluxed for 3 h under a slow purge of N_2, during which time the color changed from orange to red. A similar chromatographic separation to that above afforded compound **3** (13 mg, 52%).

Reaction of 3 with Molecular Hydrogen. Hydrogen gas was bubbled through a refluxing toluene solution (20 mL) of **3** (30 mg, 0.021 mmol) for 2 h. The solvent was removed under reduced pressure, and the residue was chromatographed by TLC on silica gel. Elution with hexane/CH_2Cl_2 (7:3, v/v) gave [Os_3 $(CO)_8(\mu$-dppf)-$(\mu$-H)$_2$] (**6**) (17 mg, 55%) as orange crystals from hexane/CH_2Cl_2 at −4 °C. Anal. calcd for $C_{44}H_{30}FeO_{10}Os_3P_2$: C, 37.56; H, 2.15. Found: C, 37.67; H, 2.24%. IR (ν(CO), CH_2Cl_2): 2064 vs, 2011 vs, 1983 vs, 1951 m cm^{-1}. ^{1}H NMR (CD_2Cl_2): δ 7.46 (m, 20H), 4.39 (s, 4H), 3.94 (s, br, 4H), −9.33 (t, J_{P-H} = 6.8 Hz; 2H). ^{31}P-{^{1}H} NMR (CD_2Cl_2): δ −7.2 (s, 2P). FAB MS: m/z 1408 (M$^+$).

Reaction of [Os$_3$ (CO)$_{10}$(μ-H)$_2$] (4) with dppf. A mixture of **4** (100 mg, 0.105 mmol) and 1,1′-*bis*(diphenylphosphino)-ferrocene (dppf) (65 mg, 0.117 mmol) in THF (30 mL) was heated to reflux under nitrogen for 4 h. A similar workup and chromatographic separation as above afforded **6** (106 mg, 64%).

Reaction of [Os$_3$(μ-H)(CO)$_8${μ-Ph$_2$PCH$_2$PPh(C$_6$H$_4$)}] (8) with dppf. A CH_2Cl_2 solution (30 mL) of compound **8** (100 mg, 0.085 mmol) and dppf (50 mg, 0.09 mmol) was stirred for 16 h at room

temperature during which time the color changed from green to orange. The solvent was evaporated to dryness, and the residue was chromatographed by TLC on silica gel. Elution with hexane/CH_2Cl_2 (7:3, v/v) gave two bands. The faster-moving band [$Os_3(CO)_9(\mu$-dppm)(κ^1-dppf) (**9**) (49 mg, 33%) as yellow crystals after recrystallization from hexane/CH_2Cl_2 at −4 °C. Anal. calcd for $C_{68}H_{50}FeO_9Os_3P_4$: C, 46.36; H, 2.86. Found: C, 46.59; H, 2.98. IR (νCO, CH_2Cl_2): 2062 vs, 2017 vs, 1992 s, 1975 s, 1960 s, 1932 m, 1911 w cm^{-1}. ^1H NMR ($CDCl_3$): δ 7.36 (m, 40H), 4.96 (s, br, 2H), 4.39 (s, 2H), 4.23 (s, 2H), 4.15 (s, 2H), 3.83 (s, 2H). $^{31}P\{^1H\}$ NMR ($CDCl_3$): δ −9.1 (s, 1P), −16.5 (s, 1P), −24.1 (d, J = 30 Hz, 1P), −27.9 (d, J = 30 Hz, 1P). MS (FAB): m/z 1762 (M^+). The slower-moving band yielded [$Os_3(CO)_8(\mu$-dppm)(κ^2-dppf)] (**10**) (65 mg, 44%) as orange crystals after recrystallization from hexane/CH_2Cl_2 at −4 °C. Anal. calcd for $C_{67}H_{50}FeO_8Os_3P_4$: C, 46.42; H, 2.91. Found: C, 46.69; H, 3.19. IR (νCO, CH_2Cl_2): 1987 s, 1956 vs, 1920 s cm^{-1}. ^1H NMR ($CDCl_3$): δ 7.41 (m, 40H), 4.87 (s, br, 2H), 4.52 (s, br, 4H), 4.31 (s, br, 4H). ^{31}P-$\{^1H\}$ NMR ($CDCl_3$): δ −7.5 (s, 2P), −32.5 (s, 2P). MS (FAB): m/z 1734 (M^+).

Reaction of [$Os_3(CO)_{10}(\mu$-dppm)] (7) with dppf. Compound **7** (150 mg, 0.121 mmol), dppf (100 mg, 0.180 mmol), and toluene (35 mL) were combined in a flame-dried 100 mL two-neck round-bottom flask. The reaction mixture was heated to reflux for 5 h. After removal of the solvent under reduced pressure, the residue was dissolved in a minimum volume of dichloromethane and chromatographed by TLC on silica gel. Elution with cyclohexane/CH_2Cl_2 (7:3, v/v) developed two bands. The faster-moving band yielded **9** (72 mg, 34%), whereas the slower-moving band gave **10** (61 mg, 29%).

Conversion of 9 to 10. A toluene solution (15 mL) of **9** (25 mg, 0.014 mmol) was refluxed for 5 h during which time the color changed from orange to red. The solvent was removed under reduced pressure and residue was taken up in CH_2Cl_2 and applied to thin-layer silica plates. Elution with hexane/CH_2Cl_2 (4:1, v/v) yielded compound **10** (20 mg, 81%).

Reaction of [$Ru_3(CO)_{12}$] with dppf. A dichloromethane solution (50 mL) of [$Ru_3(CO)_{12}$] (200 mg, 0.312 mmol) and dppf (260 mg, 0.468 mmol) was warmed to 40 °C for 1 h, and a solution of Me_3NO (50 mg, 0.667 mmol) in MeOH (4 mL) was added dropwise over a period of 15 min during which time the color changed from yellow to red. After passing through a short silica column to remove any excess Me_3NO, the solvent was removed in vacuo and the residue was dissolved in CH_2Cl_2 and applied on silica gel TLC plates. Elution with hexane/dichloromethane (7:3, v/v) developed three bands. The first two bands afforded the previously reported compounds [$Ru_3(CO)_{10}(\mu$-dppf)] (**11**) (16 mg, 10%) and [$Ru_3(CO)_8(\mu$-dppf)$_2$] (**12**) (8 mg, 5%), respectively. The third band gave [$Ru_3(CO)_8(\mu$-OH)$_2(\mu$-dppf)] (**13**) (32 mg, 20%) as orange crystals after recrystallization from CH_2Cl_2/hexane at −4 °C. Anal. calcd for $C_{42}H_{30}FeO_{10}P_2Ru_3$: C, 45.21; H, 2.71. Found: C, 45.39; H, 2.94%. IR (ν(CO), CH_2Cl_2): 2056 vs, 2008 s, 1964 vs, 1937 w cm^{-1}. ^1H NMR (CD_2Cl_2): δ 7.43 (m, 20H), 4.80 (s, br, 4H), 4.22 (s, br, 4H), −0.68 (t, J_{P-H} = 3.4 Hz, 2H). ^{31}P NMR (CD_2Cl_2): δ 2.4 (s, 2P). MS (FAB): m/z 1117 (M^+).

X-Ray Structure Determination of Compounds 2, 3, 6, and 13. Single crystals of **2**, **3**, **6**, and **13** suitable for X-ray diffraction were grown by slow diffusion of hexane into a dichloromethane solution at −4 °C. All geometric and crystallographic data for **2**, **3**, **6**, and **13** were collected at 150 K on a Bruker SMART APEX CCD diffractometer using Mo Kα radiation (λ = 0.71073 Å). Data reduction and integration were carried out with SAINT+, and absorption corrections were applied using the program SADABS.[54] Structures were solved by direct methods and developed using alternating cycles of least-squares refinement and difference Fourier synthesis. All non-hydrogen atoms were refined anisotropically. Hydrogen atoms, except those bonded to Os, were placed in the calculated positions, and their thermal parameters were linked to those of the atoms to which they were attached (riding model). Hydrogen atoms bridging Os atoms were located and their positions refined for compound **6** using fixed isotropic thermal parameters. The SHELXTL PLUS V6.10 program package was used for structure solution and refinement.[55] Final difference maps did not show any residual electron density of stereochemical significance. The details of the data collection and structure refinement are given in Table 1.

Acknowledgment. Part of this work was carried out by S.E.K. at University College London. He gratefully acknowledges the Royal Society (London) for a fellowship to spend time at UCL. We thank Dr. Dalia Rokhsana and Dr. Viktor Moberg for recording VT NMR spectra and Professor A. J. Deeming for simulation of these.

Supporting Information Available: Crystallographic data for the structural analyses have been deposited with the Cambridge Crystallographic Data Centre, CCDC Nos. 237815 for **2**, 237816 for **3**, 651078 for **6**, and 237817 for **13**. Copies of this information may be obtained free of charge from The Director, CCDC, 12 Union Road, Cambridge, CB2 1EZ, UK (fax: +44 1223 336033, E-mail: deposit@ccdc.cam.ac.uk, or on the Web at http://www.ccdc.ac.uk). This material is available free of charge via the Internet at http://pubs.acs.org.

OM700759Z

(54) *SMART and SAINT+ software for CCDC diffractometers*, version 6.1; Bruker AXS Inc.: Madison, WI, 2000.

(55) Sheldrick, G. M. *SHELXTL PLUS*, version 6; Bruker AXS: Madison, WI, 2000.